reduced cardiac hypertrophy in response to pressure overload, J. Clin. Invest. 104 (1999) 567–576.
[71] K.V. Chowdari, K. Mirnics, P. Semwal, J. Wood, E. Lawrence, T. Bhatia, S.N. Deshpande, B.K. T, R.E. Ferrell, F.A. Middleton, et al., Association and linkage analyses of RGS4 polymorphisms in schizophrenia, Hum. Mol. Genet. 11 (2002) 1373–1380.
[72] D.W. Morris, A. Rodgers, K.A. McGhee, S. Schwaiger, P. Scully, J. Quinn, D. Meagher, J.L. Waddington, M. Gill, A.P. Corvin, Confirming RGS4 as a susceptibility gene for schizophrenia, Am. J. Med. Genet. B: Neuropsychiatr. Genet. 125B (2004) 50–53.
[73] X. Chen, C. Dunham, S. Kendler, X. Wang, F.A. O'Neill, D. Walsh, K.S. Kendler, Regulator of G-protein signaling 4 (RGS4) gene is associated with schizophrenia in Irish high density families, Am. J. Med. Genet. B: Neuropsychiatr. Genet. 129B (2004) 23–26.
[74] P. Tamirisa, K.J. Blumer, A.J. Muslin, RGS4 inhibits G-protein signaling in cardiomyocytes, Circulation 99 (1999) 441–447.
[75] J.H. Rogers, A. Tsirka, A. Kovacs, K.J. Blumer, G.W. Dorn 2nd, A.J. Muslin, RGS4 reduces contractile dysfunction and hypertrophic gene induction in Galpha q overexpressing mice, J. Mol. Cell. Cardiol. 33 (2001) 209–218.
[76] S.P. Heximer, S.P. Srinivasa, L.S. Bernstein, J.L. Bernard, M.E. Linder, J.R. Hepler, K.J. Blumer, G protein selectivity is a determinant of RGS2 function, J. Biol. Chem. 274 (1999) 34253–34259.
[77] J.R. Traynor, R.R. Neubig, Regulators of G protein signaling & drugs of abuse, Mol. Interv. 5 (2005) 30–41.
[78] W. Cladman, P. Chidiac, Characterization and comparison of RGS2 and RGS4 as GTPase-activating proteins for m2 muscarinic receptor-stimulated G(i), Mol. Pharmacol. 62 (2002) 654–659.
[79] K.M. Tang, G.R. Wang, P. Lu, R.H. Karas, M. Aronovitz, S.P. Heximer, K.M. Kaltenbronn, K.J. Blumer, D.P. Siderovski, Y. Zhu, et al., Regulator of G-protein signaling-2 mediates vascular smooth muscle relaxation and blood pressure, Nat. Med. 9 (2003) 1506–1512.
[80] S.L. Grant, B. Lassegue, K.K. Griendling, M. Ushio-Fukai, P.R. Lyons, R.W. Alexander, Specific regulation of RGS2 messenger RNA by angiotensin II in cultured vascular smooth muscle cells, Mol. Pharmacol. 57 (2000) 460–467.
[81] J. Hao, C. Michalek, W. Zhang, M. Zhu, X. Xu, U. Mende, Regulation of cardiomyocyte signaling by RGS proteins: differential selectivity towards G proteins and susceptibility to regulation, J. Mol. Cell. Cardiol. 41 (2006) 51–61.
[82] W. Zhang, T. Anger, J. Su, J. Hao, X. Xu, M. Zhu, A. Gach, L. Cui, R. Liao, U. Mende, Selective loss of fine tuning of Gq/11 signaling by RGS2 protein exacerbates cardiomyocyte hypertrophy, J. Biol. Chem. 281 (2006) 5811–5820.
[83] K. Levay, J.L. Cabrera, D.K. Satpaev, V.Z. Slepak, Gbeta5 prevents the RGS7–Galphao interaction through binding to a distinct Ggamma-like domain found in RGS7 and other RGS proteins, Proc. Natl. Acad. Sci. U.S.A. 96 (1999) 2503–2507.
[84] E.R. Makino, J.W. Handy, T. Li, V.Y. Arshavsky, The GTPase activating factor for transducin in rod photoreceptors is the complex between RGS9 and type 5 G protein beta subunit, Proc. Natl. Acad. Sci. U.S.A. 96 (1999) 1947–1952.
[85] B.E. Snow, A.M. Krumins, G.M. Brothers, S.F. Lee, M.A. Wall, S. Chung, J. Mangion, S. Arya, A.G. Gilman, D.P. Siderovski, A G protein gamma subunit-like domain shared between RGS11 and other RGS proteins specifies binding to Gbeta5 subunits, Proc. Natl. Acad. Sci. U.S.A. 95 (1998) 13307–13312.
[86] P.G. Jones, S.J. Lombardi, M.I. Cockett, Cloning and tissue distribution of the human G protein beta 5 cDNA, Biochim. Biophys. Acta 1402 (1998) 288–291.
[87] C.E. Ford, N.P. Skiba, H. Bae, Y. Daaka, E. Reuveny, L.R. Shekter, R. Rosal, G. Weng, C.S. Yang, R. Iyengar, et al., Molecular basis for interactions of G protein betagamma subunits with effectors, Science 280 (1998) 1271–1274.
[88] T.M. Bonacci, J.L. Mathews, C. Yuan, D.M. Lehmann, S. Malik, D. Wu, J.L. Font, J.M. Bidlack, A.V. Smrcka, Differential targeting of Gbetagamma-subunit signaling with small molecules, Science 312 (2006) 443–446.
[89] E. Toyota, W. Chilian, D. Warltier, T. Brock, E. Ritman, VEGF is crucial for coronary collateral growth in the rat, American Heart Scientific Sessions Circulation-Supple II, 2002 (Abstract #573).
[90] C. Yuan, M. Sato, S.M. Lanier, A.V. Smrcka, Signaling by a non-dissociated complex of G Protein betagamma and alpha subunits stimulated by a receptor-independent activator of G protein signaling, AGS8, J. Biol. Chem. 282 (2007) 19938–19947.
[91] M.A. Wall, D.E. Coleman, E. Lee, J.A. Iniguez-Lluhi, B.A. Posner, A.G. Gilman, S.R. Sprang, The structure of the G protein heterotrimer Gi alpha 1 beta 1 gamma 2, Cell 83 (1995) 1047–1058.
[92] E.J. Dell, J. Connor, S. Chen, E.G. Stebbins, N.P. Skiba, D. Mochly-Rosen, H.E. Hamm, The betagamma subunit of heterotrimeric G proteins interacts with RACK1 and two other WD repeat proteins, J. Biol. Chem. 277 (2002) 49888–49895.
[93] S. Chen, B.D. Spiegelberg, F. Lin, E.J. Dell, H.E. Hamm, Interaction of Gbetagamma with RACK1 and other WD40 repeat proteins, J. Mol. Cell. Cardiol. 37 (2004) 399–406.
[94] S. Chen, E.J. Dell, F. Lin, J. Sai, H.E. Hamm, RACK1 regulates specific functions of Gbetagamma, J. Biol. Chem. 279 (2004) 17861–17868.
[95] D.H. Korzick, D.A. Holiman, M.O. Boluyt, M.H. Laughlin, E.G. Lakatta, Diminished alpha1-adrenergic-mediated contraction and translocation of PKC in senescent rat heart, Am. J. Physiol. Heart Circ. Physiol. 281 (2001) H581–589.
[96] H.C. O'Donovan, P.A. Kiely, R. O'Connor, Effects of RACK1 on cell migration and IGF-I signalling in cardiomyoctes are not dependent on an association with the IGF-IR, Cell Signal. 19 (2007) 2588–2595.
[97] S.E. Jarvis, J.M. Magga, A.M. Beedle, J.E. Braun, G.W. Zamponi, G protein modulation of N-type calcium channels is facilitated by physical interactions between syntaxin 1A and Gbetagamma, J. Biol. Chem. 275 (2000) 6388–6394.
[98] S.E. Jarvis, W. Barr, Z.P. Feng, J. Hamid, G.W. Zamponi, Molecular determinants of syntaxin 1 modulation of N-type calcium channels, J. Biol. Chem. 277 (2002) 44399–44407.
[99] Y. Kang, B. Ng, Y.M. Leung, Y. He, H. Xie, D. Lodwick, R.I. Norman, A. Tinker, R.G. Tsushima, H.Y. Gaisano, Syntaxin-1A actions on sulfonylurea receptor 2A can block acidic pH-induced cardiac K(ATP) channel activation, J. Biol. Chem. 281 (2006) 19019–19028.
[100] E.J. Yoon, T. Gerachshenko, B.D. Spiegelberg, S. Alford, H.E. Hamm, Gbetagamma interferes with Ca^{2+}-dependent binding of synaptotagmin to the soluble N-ethylmaleimide-sensitive factor attachment protein receptor (SNARE) complex, Mol. Pharmacol. 72 (2007) 1210–1219.
[101] C.G. Peters, D.F. Miller, D.R. Giovannucci, Identification, localization and interaction of SNARE proteins in atrial cardiac myocytes, J. Mol. Cell. Cardiol. 40 (2006) 361–374.
[102] R.H. Lee, B.S. Lieberman, R.N. Lolley, A novel complex from bovine visual cells of a 33,000-dalton phosphoprotein with beta- and gamma-transducin: purification and subunit structure, Biochemistry 26 (1987) 3983–3990.
[103] S. Danner, M.J. Lohse, Phosducin is a ubiquitous G-protein regulator, Proc. Natl. Acad. Sci. U.S.A. 93 (1996) 10145–10150.
[104] C. Klenk, J. Humrich, U. Quitterer, M.J. Lohse, SUMO-1 controls the protein stability and the biological function of phosducin, J. Biol. Chem. 281 (2006) 8357–8364.
[105] C. Thibault, J. Feng Wang, R. Charnas, D. Mirel, S. Barhite, M.F. Miles, Cloning and characterization of the rat and human phosducin-like protein genes: structure, expression and chromosomal localization, Biochim. Biophys. Acta 1444 (1999) 346–354.
[106] S. Schroder, M.J. Lohse, Quantification of the tissue levels and function of the G-protein regulator phosducin-like protein (PhlP), Naunyn Schmiedebergs Arch. Pharmacol. 362 (2000) 435–439.
[107] C. Thibault, M.W. Sganga, M.F. Miles, Interaction of phosducin-like protein with G protein betagamma subunits, J. Biol. Chem. 272 (1997) 12253–12256.

[108] R. Gaudet, A. Bohm, P.B. Sigler, Crystal structure at 2.4 angstroms resolution of the complex of transducin betagamma and its regulator, phosducin, Cell 87 (1996) 577–588.
[109] S. Schroder, M.J. Lohse, Inhibition of G-protein betagamma-subunit functions by phosducin-like protein, Proc. Natl. Acad. Sci. U.S.A. 93 (1996) 2100–2104.
[110] Z. Li, K.L. Laugwitz, K. Pinkernell, I. Pragst, C. Baumgartner, E. Hoffmann, K. Rosport, G. Münch, A. Moretti, J. Humrich, M.J. Lohse, M. Ungerer, Effects of two Gbetagamma-binding proteins – N-terminally truncated phosducin and beta-adrenergic receptor kinase C terminus (betaARKct) – in heart failure, Gene Ther. 10 (2003) 1354–1361.
[111] S. Li, T. Okamoto, M. Chun, M. Sargiacomo, J.E. Casanova, S.H. Hansen, I. Nishimoto, M.P. Lisanti, Evidence for a regulated interaction between heterotrimeric G proteins and caveolin, J. Biol. Chem. 270 (1995) 15693–15701.
[112] P. Oh, J.E. Schnitzer, Segregation of heterotrimeric G proteins in cell surface microdomains. G(q) binds caveolin to concentrate in caveolae, whereas G(i) and G(s) target lipid rafts by default, Mol. Biol. Cell 12 (2001) 685–698.
[113] M.H. Elliott, S.J. Fliesler, A.J. Ghalayini, Cholesterol-dependent association of caveolin-1 with the transducin alpha subunit in bovine photoreceptor rod outer segments: disruption by cyclodextrin and guanosine 5′-*O*-(3-thiotriphosphate), Biochemistry 42 (2003) 7892–7903.
[114] H.H. Patel, F. Murray, P.A. Insel, Caveolae as organizers of pharmacologically relevant signal transduction molecules, Annu. Rev. Pharmacol. Toxicol. 48 (2008) 359–391.
[115] Y. Han, Y.S. Chen, Z. Liu, N. Bodyak, D. Rigor, E. Bisping, W.T. Pu, P.M. Kang, Overexpression of HAX-1 protects cardiac myocytes from apoptosis through caspase-9 inhibition, Circ. Res. 99 (2006) 415–423.
[116] J.A. Pitcher, J. Inglese, J.B. Higgins, J.L. Arriza, P.J. Casey, C. Kim, J.L. Benovic, M.M. Kwatra, M.G. Caron, R.J. Lefkowitz, Role of beta gamma subunits of G proteins in targeting the beta-adrenergic receptor kinase to membrane-bound receptors, Science 257 (1992) 1264–1267.
[117] Y. Daaka, J.A. Pitcher, M. Richardson, R.H. Stoffel, J.D. Robishaw, R.J. Lefkowitz, Receptor and G betagamma isoform-specific interactions with G protein-coupled receptor kinases, Proc. Natl. Acad. Sci. U.S.A. 94 (1997) 2180–2185.
[118] R. Vaiskunaite, T. Kozasa, T.A. Voyno-Yasenetskaya, Interaction between the G alpha subunit of heterotrimeric G(12) protein and Hsp90 is required for G alpha(12) signaling, J. Biol. Chem. 276 (2001) 46088–46093.

Invited Review for the 2009 Hirosi Kuriyama Award

Regulation of vascular tone and remodeling of the ductus arteriosus

Utako YOKOYAMA[1], Susumu MINAMISAWA[2] and Yoshihiro ISHIKAWA[1]

[1]Cardiovascular Research Institute, Yokohama City University Graduate School of Medicine, Japan
[2]Department of Life Science and Medical Bioscience, Waseda University Graduate School of Advanced Science and Engineering, Japan

Received January 6, 2010; Accepted January 10, 2010

Abstract

The ductus arteriosus (DA), a fetal arterial connection between the main pulmonary artery and the descending aorta, normally closes immediately after birth. The DA is a normal and essential fetal structure. However, it becomes abnormal if it remains patent after birth. Closure of the DA occurs in two phases: functional closure of the lumen within the first hours after birth by smooth muscle constriction, and anatomic occlusion of the lumen over the next several days due to extensive neointimal thickening in human DA. There are several events that promote the DA constriction immediately after birth: (a) an increase in arterial oxygen tension, (b) a dramatic decline in circulating prostaglandinE_2 (PGE_2), (c) a decrease in blood pressure within the DA lumen, and (d) a decrease in the number of PGE_2 receptors in the DA wall. Anatomical closure of the DA is associated with the formation of intimal thickening, which are characterized by (a) an area of subendothelial deposition of extracellular matrix, (b) the disassembly of the internal elastic lamina and loss of elastic fiber in the medial layer, and (c) migration into the subendothelial space of undifferentiated medial smooth muscle cells. In addition to the well-known vasodilatory role of PGE_2, our findings uncovered the role of PGE_2 in anatomical closure of the DA. Chronic PGE_2-EP4-cyclic AMP (cAMP)-protein kinase A (PKA) signaling during gestation induces vascular remodeling of the DA to promote hyaluronan-mediated intimal thickening and structural closure of the vascular lumen. A novel target of cAMP, Epac, has an acute promoting effect on smooth muscle cell migration without hyaluronan production and thus intimal thickening in the DA. Both EP4-cAMP downstream targets, Epac and PKA, regulate vascular remodeling in the DA.

Key words: cyclic AMP, exchange protein activated by cyclic AMP (EPAC), protein kinase A, intimal thickening, the ductus arteriosus, vascular remodeling, hyaluronan

Correspondence to: Utako Yokoyama, MD, PhD, Cardiovascular Research Institute, Yokohama City University Graduate School of Medicine, 3-9 Fukuura Kanazawa-ku Yokohama City 236-0004, Japan
Phone: +81-45-787-2575 Fax: +81-45-788-1470 e-mail: utako@yokohama-cu.ac.jp
UY was the winner of the Hirosi Kuriyama Award.

Introduction

The ductus arteriosus (DA), a fetal arterial connection between the pulmonary artery and the descending aorta, is indispensable for fetal life. It shunts deoxygenated blood from the main pulmonary artery to the descending aorta. Over half of the blood flow in the descending aorta is diverted to the umbilico-placental circulation (Heymann and Rudolph, 1975), where gaseous exchange takes place. Although patency of the DA is required for fetal survival, the persistence of a patent DA after birth is a major cause of morbidity and mortality, especially in premature infants, leading to severe complications, including pulmonary hypertension, right ventricular dysfunction, postnatal infections and respiratory failure (Hermes-DeSantis and Clyman, 2006). The incidence of DA patency has been estimated to be one in 500 in term newborns and accounts for the majority of all cases of congenital heart diseases in preterm newborns (Mitchell *et al.*, 1971). In preterm babies with birth weights <1,500 g, the incidence of a patent DA exceeds 30% (Van Overmeire *et al.*, 2004). In addition, the presence of a patent DA is more serious in premature infants than in full-term infants since premature infants with a patent DA are more likely to develop problems such as intraventricular hemorrhage, necrotizing enterocolitis, bronchopulmonary dysplasia and congestive heart failure. Therefore, it is important to understand the precise mechanisms of regulation of the DA.

Closure of the human DA is believed to occur in two phases: (1) functional closure of the lumen within the first hours after birth by smooth muscle constriction, and (2) anatomic occlusion of the lumen over the next several days due to extensive neointimal thickening and loss of smooth muscle cells from the inner muscle media (Smith, 1998; Clyman, 2006; Yokoyama *et al.*, 2006b). Although its process is similar in mammalian DA, the time course of two phases is variable among species. There are several events that promote the DA constriction immediately after birth: (a) an increase in arterial oxygen tension, (b) a dramatic decline in circulating prostaglandinE_2 (PGE_2) because of metabolism in the now functioning lungs and elimination of the placental source, (c) a decrease in blood pressure within the DA lumen, and (d) a decrease in the number of PGE_2 receptors in the DA wall (Smith, 1998; Clyman, 2006).

The DA later undergoes permanent closure through structural remodeling and fibrosis. The resulting fibrous band with no lumen persists as the ligamentum arteriosum (Fay and Cooke, 1972). Anatomical closure of the DA is associated with the formation of intimal thickening, which are characterized by (a) an area of subendothelial deposition of extracellular matrix, (b) the disassembly of the internal elastic lamina and loss of elastic fiber in the medial layer, and (c) migration into the subendothelial space of undifferentiated medial smooth muscle cells (Smith, 1998). Some of these changes begin about halfway through gestation and some occur after functional closure of the DA in the neonate (Slomp *et al.*, 1997; Yokoyama *et al.*, 2006b). This cascade of events is thought to orchestrate the subsequent luminal DA reorganization, leading finally to complete obliteration of the DA. In this report, we review the current state of knowledge of the mechanisms of regulating vascular tone and remodeling of the DA.

1. Functional closure of the DA

1-1. Oxygen-induced contraction

During the fetal life, the DA is exposed to an oxygen tension that has been estimated as between 18 to 28 mmHg (Heymann and Rudolph, 1975). After birth, the DA is exposed to arterial blood and arterial oxygen tension rises rapidly after delivery. Rising oxygen tension significantly contracts the DA (Smith, 1998). With the exception of the pulmonary artery, most vascular smooth muscles relax in a low oxygen environment and contract in response to increasing oxygen tension. However, the response of the DA to oxygen is much greater in magnitude, although qualitatively similar to other vessels (Heymann and Rudolph, 1975; Smith and McGrath, 1988).

Several mechanisms have been proposed to explain the contractile effect of raising oxygen tension in the DA. The increase in oxygen tension inhibits ductal smooth muscle voltage-dependent potassium channels (Michelakis *et al.*, 2000; Reeve *et al.*, 2001), such as Kv1.5 and Kv2.1, which results in membrane depolarization, an influx of calcium and DA constriction (Nakanishi *et al.*, 1993; Leonhardt *et al.*, 2003). The inhibition of potassium channels is associated with production of diffusible redox mediator (H_2O_2) by a mitochondrial O_2-sensor, electron transport chain complexes I or III in the DA (Archer *et al.*, 2004). It has been reported that ATP-sensitive potassium channel was inhibited by the raising oxygen tension, resulting in membrane depolarization (Nakanishi *et al.*, 1993). In addition to involvement of potassium channels, recent study reported that depolarization-independent DA contraction is caused by release of calcium from the IP_3-sensitive store in the sarcoplasmic reticulum. Subsequent calcium entry through store-operated channels increases an influx of calcium and DA constriction (Hong *et al.*, 2006). Schematic illustration of the functional closure of the DA is shown in Figure 1.

Calcium entry trough L-type voltage-dependent calcium channels is involved in oxygen-induced DA contraction (Tristani-Firouzi *et al.*, 1996). Our previous study demonstrated that among L-type calcium channels, Cav1.2 was predominant isoform and expression level of Cav1.2 was higher in the rat DA than in the aorta (Yokoyama *et al.*, 2006a). Calcium influx through T-type voltage-dependent calcium channels, especially Cav3.1, also promoted oxygenation-induced DA constriction (Nakanishi *et al.*, 1993; Akaike *et al.*, 2009).

Coceani *et al.* reported that cytochrome P_{450} was the oxygen sensor and its activation promoted DA contraction through production of endothelin-1 (ET-1) from endothelium and smooth muscle of the DA (Coceani and Kelsey, 1991; Coceani *et al.*, 1992). They demonstrated stimulation of endothelin A receptor (ET_A) is associated with oxygen-induced DA contraction using mice with genetic disruption of ET_A (Coceani *et al.*, 1999). However, the DA was normally closed after birth in ET_A knockout mice. Consequently, ET-1- ET_A signaling plays a role in oxygen-induced contraction, but not in anatomical closure in the DA.

Vitamin A and/or retinoic acid signaling is a candidate for the activator of oxygen sensitivity, because the retinoic acid response element is strongly expressed in the mouse DA (Colbert *et al.*, 1996), and maternally administrated vitamin A accelerated development of the oxygen-sensing mechanism of the rat DA (Wu *et al.*, 2001). Our study demonstrated that

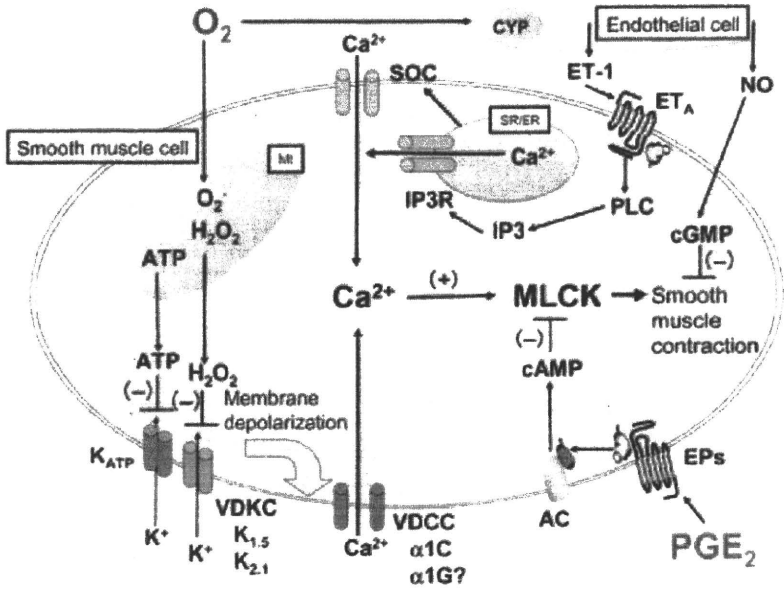

Fig. 1. A schematic model of functional closure of the DA. K^+: potassium ion, Ca^{2+}: calcium ion, O_2: oxygen, O_2^-: superoxide anion, H_2O_2: hydrogen peroxide, ATP: adenosine triphosphate, K_{ATP}: ATP-dependent potassium channel, VDCK: voltage-dependent potassium channel, VDCC: voltage-dependent calcium channel, SOC: store-operated calcium channel, Mt: mitochondria, SR/ER: sarco/endoplasmic reticulum, IP3: inositol triphosphate, IP3R: IP3 receptor, PLC: phopholipase C, MLCK: myosin light chain kinase, CYP: cytochrome P_{450}.

maternally administrated vitamin A increased the expression levels of Cav1.2 and Cav3.1 in the rat DA (Yokoyama *et al.*, 2006a).

1-2. Rapid withdrawal of the vasodilator effect of PGE_2

PGE_2 is produced in the placenta (Smith, 1998) and the DA (Clyman *et al.*, 1978; Coceani *et al.*, 1978) and contributes to the DA patency in utero. Stimulation of PGE_2 receptors activates adenylyl cyclases (Bouayad *et al.*, 2001). The increased intracellular concentrations of cyclic AMP (cAMP) inhibit myosin light chain kinase, resulting in the DA relaxation (Smith, 1998). The dilator effect of PGE_2 on the rabbit DA was mediated by the PGE_2 receptor, EP4 (Smith and McGrath, 1994). After birth, the high fetal circulating concentrations of PGE_2 dramatically decline because the placenta is removed and the lung promotes catabolism of PGE_2 (Smith, 1998). Further, the expressions of PGE_2 receptors were decreased in the DA wall (Smith, 1998; Clyman, 2006).

Both isoforms of the enzyme responsible for synthesizing PGE_2, cyclooxygenase (COX)-1 and COX-2, are expressed in the fetal DA (Takahashi *et al.*, 2000). Since COX-2 expression in the fetal DA significantly increased with advancing gestational age (Trivedi *et al.*, 2006), COX-2 inhibitor-induced DA contraction is weaker in preterm rats on the 19th day of gestation than in near-term on the 21st day (Toyoshima *et al.*, 2006). A COX inhibitor is widely used for the patent DA, however, this may not be a better therapy for premature infants with patent DA.

1-3. Other factors mediating contraction of the DA

It has been reported that nitric oxide (NO) plays a role in vasodilation of the DA. NO is synthesized by endothelial nitric oxide synthase (eNOS) in the luminal endothelium and the vasavasorum endothelium and induces relaxation of the DA through cyclic GMP (cGMP) signaling (Clyman, 2006). The relative importance of the cAMP and cGMP has been studied. Adenylyl cyclase stimulator, forskolin completely reversed the combined contractile effects of elevated oxygen tension, norepinephrin and COX inhibitor, whereas inhibition of cGMP signaling by sodium nitroprusside caused 4% of the effect of forskolin (Smith and McGrath, 1993). This implies that cAMP signaling is more important than cGMP signaling in near-term DA. On the other hand, in premature DA, the combined use of an NO synthase-inhibitor and COX inhibitor produces a much greater degree of the DA contraction than COX inhibitor alone (Seidner *et al.*, 2001).

2. Anatomical closure of the DA

2-1. Histological change during perinatal period

After birth, there is extensive remodeling of the DA wall, which leads to permanent closure of the DA. Intimal thickening, a characteristic developmental remodeling process in the DA, is required for postnatal DA closure (Rabinovitch, 1996; Mason *et al.*, 1999; Yokoyama *et al.*, 2006b). Intimal thickening starts with lifting of the endothelial cells (Gittenberger-de Groot *et al.*, 1985) and accumulations of hyaluronan in the subendothelial region, creating a space that is suitable for migration of smooth muscle cells through the fragmented elastic lamina into the subentothelial region (De Reeder *et al.*, 1988). Figure 2 shows histological change of the rat DA. Intimal thickening is developed in mature rat DA on the 21st day of gestation, while it is lacked in immature DA on the19th day of gestation. Since intimal thickening is poorly developed in human patent DA patients and animal models of patent DA (Gittenberger-de Groot *et al.*, 1980; Gittenberger-de Groot *et al.*, 1985; Tada *et al.*, 1985), this process plays an important role in permanent closure of the DA after birth.

2-2. Molecular mechanisms of regulating intimal thickening

PGE_2 plays a primary role in maintaining the patency of DA, however, previous studies have demonstrated that genetic disruption of the PGE receptor EP4 paradoxically results in fatal patent DA in mice (Nguyen *et al.*, 1997; Segi *et al.*, 1998). In addition, double mutant mice in which COX-1 and COX-2 are disrupted also exhibit patent DA (Loftin *et al.*, 2001). We found that intimal thickening was completely absent in the DA from EP4-disrupted neonatal mice (Yokoyama *et al.*, 2006b). Moreover, a marked reduction in hyaluronan production was found in EP4-disrupted DA, whereas a thick layer of hyaluronan deposit was present in wile-type DA. PGE_2-EP4-cAMP-protein kinase A (PKA) signaling up-regulates hyaluronan synthase type 2 mRNA, which increases hyaluronan production in the DA. Accumulation of hyaluronan then promotes smooth muscle cell migration into the subendothelial layer to form intimal thickening (Yokoyama *et al.*, 2006b). Signals through PGE_2-EP4 have two essential roles in DA development, namely, vascular dilation and intimal thickening.

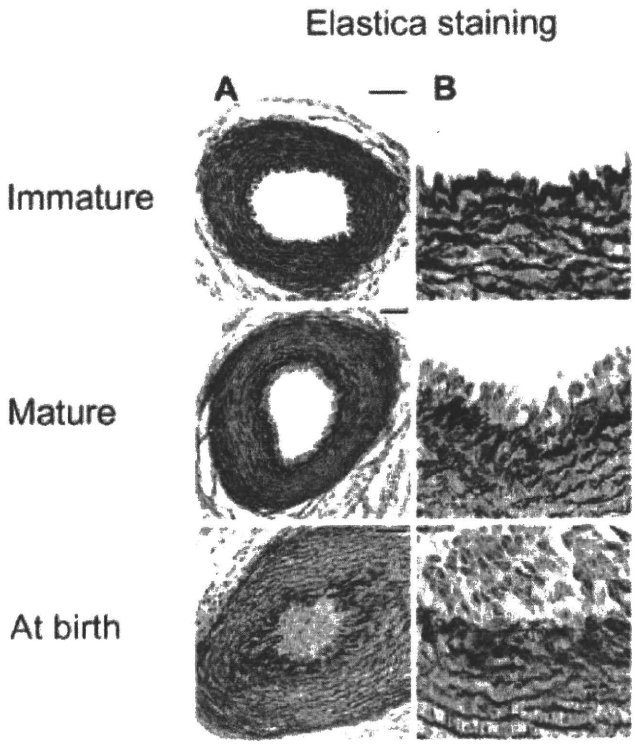

Fig. 2. Developmental changes in intimal thickening in rat DA. (A) Elastica van Gieson staining shows that intimal thickening was poor on the 19th day of gestation (immature), whereas it became apparent on the 21st day of gestation (mature) and 4 hours after birth (at birth). (B) DA intimal thickening are also shown at higher magnification.

A new target of cAMP, *i.e.*, an exchange protein activated by cAMP, has recently been discovered; it is called Epac (de Rooij *et al.*, 1998). Epac has been known to exhibit a distinct cAMP signaling pathway that is independent of PKA (Bos, 2003). Our previous study demonstrated that Epac, which is up-regulated during the perinatal period, had an acute promoting effect on smooth muscle cell migration without hyaluronan production and thus intimal thickening in the DA (Yokoyama *et al.*, 2008). Therefore, both EP4-cAMP downstream targets, Epac and PKA, induced intimal thickening in the DA (Fig. 3).

T-type voltage-dependent calcium channels, especially Cav3.1, promoted oxygenation-induced DA constriction (Akaike *et al.*, 2009). Our study revealed that Cav3.1 was significantly up-regulated in oxygenated rat DA tissue and in the region of intimal thickening of DA and that Cav1.3 promoted smooth muscle cell migration. These results indicate that Cav1.3 promotes oxygenation-induced DA closure through smooth muscle cell migration and vasoconstriction in rats (Akaike *et al.*, 2009). We also found that a novel spliced variant of the alpha1C-subunit was highly expressed in the neointima cushion of the DA (Yokoyama *et al.*, 2006a), although a role of the novel isoform is needed to be studied.

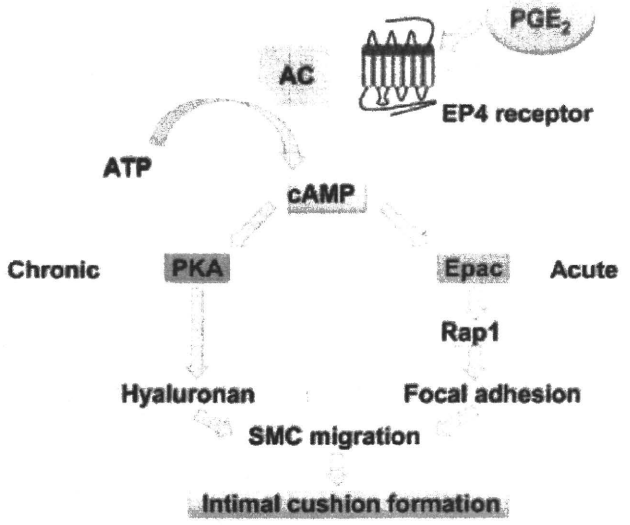

Fig. 3. A schematic model of the diverse cAMP signaling pathway. Both Epac and PKA synergistically promoted intimal cushion formation in the DA, but they work in two distinct ways: Epac-mediated (acute) and PKA-mediated (chronic) promotion. AC: adenylyl cyclase.

2-3. Extracellular matrix in the DA

Vascular cells are defined by the ways in which they regulate their extracellular matrix, and changes in the extracellular matrix, in turn, determine vascular cell phenotype, *i.e.*, the ability to differentiate, proliferate, and migrate (Rabinovitch, 1996). It has been reported that DA smooth muscle cells produce two-fold more fibronectin than aortic smooth muscle cells (Rabinovitch, 1996). Mason *et al.* have demonstrated that preventing fibronectin-dependent intimal thickening would be a feasible manipulation to cause patent DA as a mode of treatment of congenital heart diseases (Mason *et al.*, 1999). Our previous study also demonstrated that maternally administrated viamin A increased fibronectin production and intimal thickening in the rat DA (Yokoyama *et al.*, 2007). Transforming growth factor beta and NO induce extracellular matrix including hyaluronan and fibronectin in DA smooth muscle cell (Rabinovitch, 1996).

Versican, an hyaluronan binding proteoglycan, plays an important role in proliferation and migration of vascular smooth muscle cells (Evanko *et al.*, 1999). Tanacin, a hexameric glycoprotein, also has been known to regulate vascular smooth muscle cell proliferation (Cowan *et al.*, 2000). Therefore, fibronectin and hyaluronan may not be the sole constituents of extracellular matrix in DA intimal thickening.

Closing remarks

The ductal closure occurs in two phases. During first few hours after birth in term newborns, there is acute and functional closure as a result of smooth muscle contraction of the

DA, which is triggered by an increase in oxygen tension and a decline in levels of circulating PGE_2. Importantly, prior to this, anatomical luminal narrowing develops through intimal thickening that occludes the vascular lumen and results in permanent closure after birth. Both PGE_2-EP4-cAMP downstream targets, Epac and PKA, induce intimal thickening in the DA. Chronic activation of EP4 induces hyaluronan-mediated smooth muscle cell migration via PKA, resulting in intimal thickening. Epac has an acute promoting effect on smooth muscle cell migration without hyaluronan production and thus intimal thickening in the DA.

Acknowledgements

This work was supported by grants from the Grant-in-Aid for Scientific Research (KAKENHI) (U.Y.), the Ministry of Health Labor and Welfare (S.M., Y.I.), the Ministry of Education, Culture, Sports, Science and Technology of Japan (S.M., Y.I.), the Yokohama Foundation for Advanced Medical Science (U.Y., S.M.), the Kanae Foundation for the Promotion for Medical Science (U.Y.), the Miyata Cardiology Research Promotion Founds (U.Y., S.M.), the Takeda Science Foundation (U.Y., S.M.), the Sumitomo Foundation (U.Y.), the Japan Heart Foundation Research Grant (U.Y.), the Kowa Life Science Foundation (U.Y.), the Cosmetology Research Foundation (Y.I.), the Uehara Memorial Foundation (U.Y.), the Kitsuen Research Foundation (Y.I.), "High-Tech Research Center" Project for Private Universities: MEXT (S.M.), Waseda University Grant for Special Research Projects (S.M.), The Vehicle Racing Commemorative Foundation (S.M.), and the Japan Space Forum (Y.I.).

References

Akaike, T., Jin, M.H., Yokoyama, U., Izumi-Nakaseko, H., Jiao, Q., Iwasaki, S., Iwamoto, M., Nishimaki, S., Sato, M., Yokota, S., Kamiya, Y., Adachi-Akahane, S., Ishikawa, Y. and Minamisawa, S. (2009). T-type Ca^{2+} channels promote oxygenation-induced closure of the rat ductus arteriosus not only by vasoconstriction but also by neointima formation. *J. Biol. Chem.* **284**: 24025–24034.

Archer, S.L., Wu, X.C., Thebaud, B., Moudgil, R., Hashimoto, K. and Michelakis, E.D. (2004). O2 sensing in the human ductus arteriosus: redox-sensitive K^+ channels are regulated by mitochondria-derived hydrogen peroxide. *Biol. Chem.* **385**: 205–216.

Bos, J.L. (2003). Epac: a new cAMP target and new avenues in cAMP research. *Nat. Rev. Mol. Cell Biol.* **4**: 733–738.

Bouayad, A., Kajino, H., Waleh, N., Fouron, J.C., Andelfinger, G., Varma, D.R., Skoll, A., Vazquez, A., Gobeil, F., Jr., Clyman, R.I. and Chemtob, S. (2001). Characterization of PGE_2 receptors in fetal and newborn lamb ductus arteriosus. *Am. J. Physiol.* **280**: H2342–H2349.

Clyman, R.I. (2006). Mechanisms regulating the ductus arteriosus. *Biol. Neonate* **89**: 330–335.

Clyman, R.I., Mauray, F., Roman, C. and Rudolph, A.M. (1978). PGE_2 is a more potent vasodilator of the lamb ductus arteriosus than is either PGI2 or 6 keto PGF1alpha. *Prostaglandins* **16**: 259–264.

Coceani, F., Bodach, E., White, E., Bishai, I. and Olley, P.M. (1978). Prostaglandin I_2 is less relaxant than prostaglandin E2 on the lamb ductus arteriosus. *Prostaglandins* **15**: 551–556.

Coceani, F. and Kelsey, L. (1991). Endothelin-1 release from lamb ductus arteriosus: relevance to postnatal closure of the vessel. *Can. J. Physiol. Pharmacol.* **69**: 218–221.

Coceani, F., Kelsey, L. and Seidlitz, E. (1992). Evidence for an effector role of endothelin in closure of the ductus arteriosus at birth. *Can. J. Physiol. Pharmacol.* **70**: 1061–1064.

Coceani, F., Liu, Y., Seidlitz, E., Kelsey, L., Kuwaki, T., Ackerley, C. and Yanagisawa, M. (1999). Endothelin A receptor is necessary for O(2) constriction but not closure of ductus arteriosus. *Am. J. Physiol.* **277**: H1521–H1531.

Colbert, M.C., Kirby, M.L. and Robbins, J. (1996). Endogenous retinoic acid signaling colocalizes with advanced expression of the adult smooth muscle myosin heavy chain isoform during development of the ductus arteriosus. *Circ. Res.* **78**: 790–798.

Cowan, K.N., Jones, P.L. and Rabinovitch, M. (2000). Elastase and matrix metalloproteinase inhibitors induce regression, and tenascin-C antisense prevents progression, of vascular disease. *J. Clin. Invest.* **105**: 21–34.

De Reeder, E.G., Girard, N., Poelmann, R.E., Van Munsteren, J.C., Patterson, D.F. and Gittenberger-De Groot, A.C. (1988). Hyaluronic acid accumulation and endothelial cell detachment in intimal thickening of the vessel wall. The normal and genetically defective ductus arteriosus. *Am. J. Pathol.* **132**: 574–585.

de Rooij, J., Zwartkruis, F.J., Verheijen, M.H., Cool, R.H., Nijman, S.M., Wittinghofer, A. and Bos, J.L. (1998). Epac is a Rap1 guanine-nucleotide-exchange factor directly activated by cyclic AMP. *Nature* **396**: 474–477.

Evanko, S.P., Angello, J.C. and Wight, T.N. (1999). Formation of hyaluronan- and versican-rich pericellular matrix is required for proliferation and migration of vascular smooth muscle cells. *Arterioscler. Thromb. Vasc. Biol.* **19**: 1004–1013.

Fay, F.S. and Cooke, P.H. (1972). Guinea pig ductus arteriosus. II. Irreversible closure after birth. *Am. J. Physiol.* **222**: 841–849.

Gittenberger-de Groot, A.C., Strengers, J.L., Mentink, M., Poelmann, R.E. and Patterson, D.F. (1985). Histologic studies on normal and persistent ductus arteriosus in the dog. *J. Am. Coll. Cardiol.* **6**: 394–404.

Gittenberger-de Groot, A.C., van Ertbruggen, I., Moulaert, A.J. and Harinck, E. (1980). The ductus arteriosus in the preterm infant: histologic and clinical observations. *J. Pediatr.* **96**: 88–93.

Hermes-DeSantis, E.R. and Clyman, R.I. (2006). Patent ductus arteriosus: pathophysiology and management. *J. Perinatol.* **26 Suppl. 1**: S14–18; discussion S22–13.

Heymann, M.A. and Rudolph, A.M. (1975). Control of the ductus arteriosus. *Physiol. Rev.* **55**: 62–78.

Hong, Z., Hong, F., Olschewski, A., Cabrera, J.A., Varghese, A., Nelson, D.P. and Weir, E.K. (2006). Role of store-operated calcium channels and calcium sensitization in normoxic contraction of the ductus arteriosus. *Circulation* **114**: 1372–1379.

Leonhardt, A., Glaser, A., Wegmann, M., Schranz, D., Seyberth, H. and Nusing, R. (2003). Expression of prostanoid receptors in human ductus arteriosus. *Br. J. Pharmacol.* **138**: 655–659.

Loftin, C.D., Trivedi, D.B., Tiano, H.F., Clark, J.A., Lee, C.A., Epstein, J.A., Morham, S.G., Breyer, M.D., Nguyen, M., Hawkins, B.M., Goulet, J.L., Smithies, O., Koller, B.H. and Langenbach, R. (2001). Failure of ductus arteriosus closure and remodeling in neonatal mice deficient in cyclooxygenase-1 and cyclooxygenase-2. *Proc. Natl. Acad. Sci. USA* **98**: 1059–1064.

Mason, C.A., Bigras, J.L., O'Blenes, S.B., Zhou, B., McIntyre, B., Nakamura, N., Kaneda, Y. and Rabinovitch, M. (1999). Gene transfer in utero biologically engineers a patent ductus arteriosus in lambs by arresting fibronectin-dependent neointimal formation. *Nat. Med.* **5**: 176–182.

Michelakis, E., Rebeyka, I., Bateson, J., Olley, P., Puttagunta, L. and Archer, S. (2000). Voltage-gated potassium channels in human ductus arteriosus. *Lancet* **356**: 134–137.

Mitchell, S.C., Korones, S.B. and Berendes, H.W. (1971). Congenital heart disease in 56,109 births. Incidence and natural history. *Circulation* **43**: 323–332.

Nakanishi, T., Gu, H., Hagiwara, N. and Momma, K. (1993). Mechanisms of oxygen-induced contraction of ductus arteriosus isolated from the fetal rabbit. *Circ. Res.* **72**: 1218–1228.

Nguyen, M., Camenisch, T., Snouwaert, J.N., Hicks, E., Coffman, T.M., Anderson, P.A., Malouf, N.N. and Koller, B.H. (1997). The prostaglandin receptor EP4 triggers remodelling of the

cardiovascular system at birth. *Nature* **390**: 78–81.

Rabinovitch, M. (1996). Cell-extracellular matrix interactions in the ductus arteriosus and perinatal pulmonary circulation. *Semin. Perinatol.* **20**: 531–541.

Reeve, H.L., Tolarova, S., Nelson, D.P., Archer, S. and Weir, E.K. (2001). Redox control of oxygen sensing in the rabbit ductus arteriosus. *J. Physiol. (Lond.)* **533**: 253–261.

Segi, E., Sugimoto, Y., Yamasaki, A., Aze, Y., Oida, H., Nishimura, T., Murata, T., Matsuoka, T., Ushikubi, F., Hirose, M., Tanaka, T., Yoshida, N., Narumiya, S. and Ichikawa, A. (1998). Patent ductus arteriosus and neonatal death in prostaglandin receptor EP4-deficient mice. *Biochem. Biophys. Res. Commun.* **246**: 7–12.

Seidner, S.R., Chen, Y.Q., Oprysko, P.R., Mauray, F., Tse, M.M., Lin, E., Koch, C. and Clyman, R.I. (2001). Combined prostaglandin and nitric oxide inhibition produces anatomic remodeling and closure of the ductus arteriosus in the premature newborn baboon. *Pediatr. Res.* **50**: 365–373.

Slomp, J., Gittenberger-de Groot, A.C., Glukhova, M.A., Conny van Munsteren, J., Kockx, M.M., Schwartz, S.M. and Koteliansky, V.E. (1997). Differentiation, dedifferentiation, and apoptosis of smooth muscle cells during the development of the human ductus arteriosus. *Arterioscler. Thromb. Vasc. Biol.* **17**: 1003–1009.

Smith, G.C. (1998). The pharmacology of the ductus arteriosus. *Pharmacol. Rev.* **50**: 35–58.

Smith, G.C. and McGrath, J.C. (1988). Indomethacin, but not oxygen tension, affects the sensitivity of isolated neonatal rabbit ductus arteriosus, but not aorta, to noradrenaline. *Cardiovasc. Res.* **22**: 910–915.

Smith, G.C. and McGrath, J.C. (1993). Characterisation of the effect of oxygen tension on response of fetal rabbit ductus arteriosus to vasodilators. *Cardiovasc. Res.* **27**: 2205–2211.

Smith, G.C. and McGrath, J.C. (1994). Interactions between indomethacin, noradrenaline and vasodilators in the fetal rabbit ductus arteriosus. *Br. J. Pharmacol.* **111**: 1245–1251.

Tada, T., Wakabayashi, T., Nakao, Y., Ueki, R., Ogawa, Y., Inagawa, A., Shibata, T. and Kishimoto, H. (1985). Human ductus arteriosus. A histological study on the relation between ductal maturation and gestational age. *Acta Pathol. Jpn.* **35**: 23–34.

Takahashi, Y., Roman, C., Chemtob, S., Tse, M.M., Lin, E., Heymann, M.A. and Clyman, R.I. (2000). Cyclooxygenase-2 inhibitors constrict the fetal lamb ductus arteriosus both in vitro and in vivo. *Am. J. Physiol.* **278**: R1496–R1505.

Toyoshima, K., Takeda, A., Imamura, S., Nakanishi, T. and Momma, K. (2006). Constriction of the ductus arteriosus by selective inhibition of cyclooxygenase-1 and -2 in near-term and preterm fetal rats. *Prostaglandins Other. Lipid Mediat.* **79**: 34–42.

Tristani-Firouzi, M., Reeve, H.L., Tolarova, S., Weir, E.K. and Archer, S.L. (1996). Oxygen-induced constriction of rabbit ductus arteriosus occurs via inhibition of a 4-aminopyridine-, voltage-sensitive potassium channel. *J. Clin. Invest.* **98**: 1959–1965.

Trivedi, D.B., Sugimoto, Y. and Loftin, C.D. (2006). Attenuated cyclooxygenase-2 expression contributes to patent ductus arteriosus in preterm mice. *Pediatr. Res.* **60**: 669–674.

Van Overmeire, B., Allegaert, K., Casaer, A., Debauche, C., Decaluwe, W., Jespers, A., Weyler, J., Harrewijn, I. and Langhendries, J.P. (2004). Prophylactic ibuprofen in premature infants: a multicentre, randomised, double-blind, placebo-controlled trial. *Lancet* **364**: 1945–1949.

Wu, G.R., Jing, S., Momma, K. and Nakanishi, T. (2001). The effect of vitamin A on contraction of the ductus arteriosus in fetal rat. *Pediatr. Res.* **49**: 747–754.

Yokoyama, U., Minamisawa, S., Adachi-Akahane, S., Akaike, T., Naguro, I., Funakoshi, K., Iwamoto, M., Nakagome, M., Uemura, N., Hori, H., Yokota, S. and Ishikawa, Y. (2006a). Multiple transcripts of Ca2+ channel alpha1-subunits and a novel spliced variant of the alpha1C-subunit in rat ductus arteriosus. *Am. J. Physiol.* **290**: H1660–H1670.

Yokoyama, U., Minamisawa, S., Quan, H., Akaike, T., Suzuki, S., Jin, M., Jiao, Q., Watanabe, M., Otsu, K., Iwasaki, S., Nishimaki, S., Sato, M. and Ishikawa, Y. (2008). Prostaglandin E2-activated Epac

promotes neointimal formation of the rat ductus arteriosus by a process distinct from that of cAMP-dependent protein kinase A. *J. Biol. Chem.* **283**: 28702–28709.

Yokoyama, U., Minamisawa, S., Quan, H., Ghatak, S., Akaike, T., Segi-Nishida, E., Iwasaki, S., Iwamoto, M., Misra, S., Tamura, K., Hori, H., Yokota, S., Toole, B.P., Sugimoto, Y. and Ishikawa, Y. (2006b). Chronic activation of the prostaglandin receptor EP4 promotes hyaluronan-mediated neointimal formation in the ductus arteriosus. *J. Clin. Invest.* **116**: 3026–3034.

Yokoyama, U., Sato, Y., Akaike, T., Ishida, S., Sawada, J., Nagao, T., Quan, H., Jin, M., Iwamoto, M., Yokota, S., Ishikawa, Y. and Minamisawa, S. (2007). Maternal vitamin A alters gene profiles and structural maturation of the rat ductus arteriosus. *Physiol. Genomics* **31**: 139–157.

THE JOURNAL OF BIOLOGICAL CHEMISTRY VOL. 286, NO. 20, pp. 17766–17776, May 20, 2011

Identification of Transcription Factor E3 (TFE3) as a Receptor-independent Activator of $G\alpha_{16}$

GENE REGULATION BY NUCLEAR Gα SUBUNIT AND ITS ACTIVATOR[*][S]

Received for publication, January 8, 2011, and in revised form, March 7, 2011 Published, JBC Papers in Press, March 24, 2011, DOI 10.1074/jbc.M111.219816

Motohiko Sato[‡1], Masahiro Hiraoka[‡], Hiroko Suzuki[‡], Yunzhe Bai[‡], Reiko Kurotani[‡], Utako Yokoyama[‡], Satoshi Okumura[‡], Mary J. Cismowski[§], Stephen M. Lanier[¶], and Yoshihiro Ishikawa[‡2]

From the [‡]Cardiovascular Research Institute, Yokohama City University School of Medicine, Fukuura, Yokohama 236-0004, Japan, [§]Center for Cardiovascular and Pulmonary Research, Research Institute at Nationwide Children's Hospital, Columbus, Ohio 43205, and [¶]Department of Pharmacology, Medical University of South Carolina, Charleston, South Carolina 29425

Receptor-independent G-protein regulators provide diverse mechanisms for signal input to G-protein-based signaling systems, revealing unexpected functional roles for G-proteins. As part of a broader effort to identify disease-specific regulators for heterotrimeric G-proteins, we screened for such proteins in cardiac hypertrophy using a yeast-based functional screen of mammalian cDNAs as a discovery platform. We report the identification of three transcription factors belonging to the same family, transcription factor E3 (TFE3), microphthalmia-associated transcription factor, and transcription factor EB, as novel receptor-independent activators of G-protein signaling selective for $G\alpha_{16}$. TFE3 and $G\alpha_{16}$ were both up-regulated in cardiac hypertrophy initiated by transverse aortic constriction. In protein interaction studies *in vitro*, TFE3 formed a complex with $G\alpha_{16}$ but not with $G\alpha_{i3}$ or $G\alpha_s$. Although increased expression of TFE3 in heterologous systems had no influence on receptor-mediated $G\alpha_{16}$ signaling at the plasma membrane, TFE3 actually translocated $G\alpha_{16}$ to the nucleus, leading to the induction of claudin 14 expression, a key component of membrane structure in cardiomyocytes. The induction of claudin 14 was dependent on both the accumulation and activation of $G\alpha_{16}$ by TFE3 in the nucleus. These findings indicate that TFE3 and $G\alpha_{16}$ are up-regulated under pathologic conditions and are involved in a novel mechanism of transcriptional regulation via the relocalization and activation of $G\alpha_{16}$.

Heterotrimeric G-proteins play key roles in transducing cell surface stimuli to intracellular signaling events (1, 2). Activation of G-protein coupled receptors (GPCRs)[3] at the cell surface initiates nucleotide exchange on Gα subunits, leading to a conformational change in $G\alpha\beta\gamma$ and subsequent transduction of signals to various intracellular effector molecules. In addition to the basic components of the G-protein signaling system (*i.e.* GPCRs, heterotrimeric G-proteins, and effector molecules), there is a novel class of regulatory proteins for heterotrimeric G-proteins that directly regulate the activation status of heterotrimeric G-proteins independently of GPCRs (3–10).

Such receptor-independent G-protein regulators are involved in unexpected and important functional roles of heterotrimeric G-proteins in multiple cellular events. For example, LGN (activator of G-protein signaling 5 (AGS5)) and AGS3 are involved in the regulation of mitotic spindle dynamics and cell division (11–14). The GTPase-activating protein RGS14 also translocates between the nucleus and the cytoplasm and is associated with centrosomes influencing mitosis (15). Another RGS protein, RGS7, interacts with $G\beta_5$ and migrates into the nucleus as an RGS7-$G\beta_5$ complex (16). Furthermore, signal alteration by G-protein and their various types of regulators is involved in adaptation of cells to maintain homeostasis under pathologic conditions (17–21). In fact, the expression of such regulatory proteins is altered with the development of cardiac hypertrophy in hypertension or in response to pressure overload stress (22, 23).

As part of a broader approach to identify adaptation-specific regulatory proteins for heterotrimeric G-proteins, we previously identified AGS8 from a cDNA library of rat hearts subjected to repetitive transient ischemia (18). AGS8 was up-regulated in cardiomyocytes in response to transient hypoxia and regulated $G\beta\gamma$ signaling. Indeed, AGS8 played a key role in apoptosis of cardiomyocytes induced by hypoxic stress via $G\beta\gamma$ and the channel protein connexin 43 (24). These findings prompted us to investigate the presence of putative AGS proteins in other models of cardiovascular diseases.

We first screened for regulatory proteins for heterotrimeric G-proteins involved in the development of cardiac

* This work was supported, in whole or in part, by National Institutes of Health Grants NS24821 and DA025896 (both to S. M. L.). This work was also supported by Grants-in-aid for Scientific Research (C) 18599006 and 20590212, the Yokohama Foundation for Advancement of Medical Science, and Strategic Research Project Grants K18017 and K19021 from Yokohama City University, Japan (all to M. S.) and by grants from the Ministry of Health Labor and Welfare; Ministry of Education, Culture, Sports, Science and Technology of Japan; Takeda Science Foundation; Cosmetology Research Foundation; and Kitsuen Research Foundation (all to Y. I.).

[S] The on-line version of this article (available at http://www.jbc.org) contains supplemental Figs. 1 and 2 and Text 1–3.

[1] Supported by the Takeda Science Foundation, the NOVARTIS Foundation (Japan) for the Promotion of Science, the Mitsubishi Pharma Research Foundation, The Ichiro Kanehara Foundation, and the Mochida Memorial Foundation for Medical and Pharmaceutical Research. To whom correspondence may be addressed: Cardiovascular Research Inst., Yokohama City University School of Medicine, 3-9 Fukuura, Kanazawa-Ku, Yokohama 236-0004, Japan. Fax: 81-45-788-1470; E-mail: motosato@yokohama-cu.ac.jp.

[2] To whom correspondence may be addressed. E-mail: yishikaw@med.yokohama-cu.ac.jp.

[3] The abbreviations used are: GPCR, G-protein coupled receptor; TFE, transcription factor E; MITF, microphthalmia-associated transcription factor; TFEB, transcription factor EB; AGS, activators of G-protein signaling; RGS, regulator of G protein signaling; TAC, transverse aortic constriction; PLC, phospholipase C.

hypertrophy. Cardiac hypertrophy is a gateway to cardiac dysfunction and acts as an independent risk factor for cardiovascular events. GPCR-mediated signaling pathways, in particular those involving β-adrenergic or angiotensin II receptors, influence gene expression involved in cardiac hypertrophy. Overexpression of $G\alpha_s$ or $G\alpha_q$ in the mouse heart actually results in the development of cardiac hypertrophy and dysfunction.

We report the identification of three $G\alpha_{16}$-selective AGS proteins using a yeast-based discovery platform for receptor-independent activators of G-protein signaling to screen cDNA libraries from mouse models of cardiac hypertrophy induced by transverse aortic constriction (TAC) or continuous infusion of the β-adrenergic agonist isoproterenol. Of importance, the three new AGS proteins are microphthalmia-associated transcription factor (MITF)/TFE transcription factors. Although increased expression of TFE3 in heterologous systems had no influence on receptor-mediated $G\alpha_{16}$ signaling at the plasma membrane, TFE3 actually translocated $G\alpha_{16}$ to the nucleus, leading to the induction of claudin 14, a key component of membrane structure in cardiomyocytes. These findings indicate that $G\alpha_{16}$-selective AGS proteins are up-regulated under pathologic conditions and are involved in a novel mechanism of transcriptional regulation via the relocalization and activation of $G\alpha_{16}$.

EXPERIMENTAL PROCEDURES

Materials

Anti-$G\alpha_{i3}$, anti-$G\alpha_s$, and anti-phospholipase C (PLC)-β2 antibodies and anti-β_2-adrenergic receptor were purchased from Santa Cruz Biotechnology. IGEPAL CA-630 and anti-β-actin antibody were obtained from Sigma. Anti-$G\alpha_{16}$ and anti-claudin 14 antibodies were purchased from Medical and Biological Laboratories, Co., Ltd. (Nagoya, Japan) and Abcam, respectively. Anti-Xpress antibody and Lipofectamine 2000 reagent were obtained from Invitrogen. pcDNA3.1::$G\alpha_{16}$ and pcDNA3.1::$G\alpha_{16}$Q212L were obtained from the Missouri S&T cDNA Resource Center. $G\alpha_{16}$G211A was generated by site-direct mutagenesis (PrimeSTAR Mutagenesis Basal kit, Takara, Otsu, Japan). Full-length mouse TFE3, human transcription factor EB (TFEB), and mouse MITF were subcloned into the pYES2 vector (Invitrogen) or pcDNAHis vector (Invitrogen) from cDNA clones (Open Biosystems) (TFE3, MMM1013-98478992; TFEB, MHS1010-7508073; MITF, EMM1002-97035453).

Animal Models

All animal experiments were performed according to procedures approved by the Institutional Animal Care and Use Committee at Yokohama City University.

TAC—Constriction of the transverse thoracic aorta was performed on 14 male mice (C57BL/6; age, 14–17 weeks; 24–29 g; Charles River Laboratories, Gilroy, CA) as described previously (25). In brief, mice were anesthetized, intubated, and placed on a respirator. The transverse aorta was visualized following midline sternotomy. A 5-0 nylon suture was placed around the aorta distal to the brachiocephalic artery. The suture was tightened around a blunt 27-gauge needle placed adjacent to the aorta to produce −70% constriction. The needle was then removed, and the chest and overlying skin were closed. Six age-matched animals underwent the same surgical procedure but without TAC (sham). Seven days after surgery, the mice were sacrificed for tissue extraction. The left ventricles were quickly separated, frozen in liquid nitrogen, and stored at −70 °C until use.

Cardiac Hypertrophy and Tachycardia—Nineteen male mice (C57BL/6; age, 16–19 weeks; 25–30 g; Charles River Laboratories) were anesthetized, and an osmotic minipump (model 2002, ALZET Osmotic Pumps, Cupertino, CA) was implanted subcutaneously (18). After 7 days of continuous infusion of isoproterenol (60 μg/g of body weight/day), mice were anesthetized, and the hearts were rapidly excised. The left ventricles were rapidly frozen in liquid nitrogen and stored at −70 °C until use.

Generation of cDNA Libraries and Functional Screen in Saccharomyces cerevisiae

mRNA isolated from the left ventricle in the TAC or tachycardia models was used to synthesize cDNAs using a cDNA Synthesis kit (Takara); cDNAs were cloned into the pYES2 yeast expression vector. The cDNA library from the TAC model contained 1.1×10^6 cfu with an average insert size of 1.5 kb, and the library from tachycardia model contained 2.8×10^6 cfu with an average insert size of 1.2 kb. Functional screens and growth assays in the modified strains of *S. cerevisiae* were conducted as described previously (26–28).

Quantitative Polymerase Chain Reaction (PCR)

RNA isolation, cDNA synthesis, and real time PCR analysis were performed as described previously (24). The primers for RT-PCR were as follows: mouse MITF: forward, 5′-ACTTTCCCTTATCCCATCCACC-3′; reverse, 5′-TGAGATCCAGAGTTGTCGTACA-3′; mouse TFE3: forward, 5′-TGCGTCAGCAGCTTATGAGG-3′; reverse, 5′-AGACACGCCAATCACAGAGAT-3′; mouse TFEB: forward, 5′-CCACCCCAGCCATCAACAC-3′; reverse, 5′-CAGACAGATACTCCCGAACCTT-3′; mouse GNA15: forward, 5′-CGCCAGAATCGACCAGGAG-3′; reverse, 5′-GTAGCCCACACCGTGAATGA-3′; mouse claudin 14: forward, 5′-GCATGGTGGGAACGCTCAT-3′; reverse, 5′-CCACAGTCCCTTCAGGTAGGA-3′; human claudin 14: forward, 5′-CAAACACCGCACCTGCCTA-3′; reverse, 5′-CACGTAGTCGTTCAGCCTGT-3′; rat GNA15: forward, 5′-CAGGAGAACCGTATGAAGGAGAGTC-3′; reverse, 5′-CAGGATGTCTGTCTTGTTGAGGAAG-3′; rat TFE3: forward, 5′-TGTTCGTGCTGTTGGAAGAGC-3′; reverse, 5′-GGGATAGAGGCTGGCTTTTGAG-3′; rat claudin 14: forward, 5′-TCATCACTACTATCCTGCCGCAC-3′; reverse, 5′-ACACACTCCATCCACAGTCCCTTC-3′; and 18 S: forward, 5′-GTAACCCGTTGAACCCCATT-3′; reverse, 5′-CCATCCAATCGGTAGTAGCG-3′. All PCRs were performed in duplicate or triplicate at 95 °C for 2 min followed by 40 cycles at 95 °C for 30 s and 60 or 62 °C for 45 s. The cycle threshold values corresponding to the PCR cycle number at which fluorescence emission in real time reaches a threshold above the base-line emission were determined. 18 S ribosomal

RNA was used as a control for the amount of target mRNA in each sample.

Generation of Glutathione S-Transferase (GST) Fusion Protein, Protein Interaction Assays, and Immunoblotting

The coding sequence of TFE3 (amino acids Leu^{40}–Ser^{572}; cDNA1-8) was amplified by PCR and fused in-frame to GST in the pGEX-6T vector (Amersham Biosciences). The GST-TFE3 fusion protein was expressed in bacteria (*Escherichia coli* BL21; Amersham Biosciences) and purified on a glutathione affinity matrix. The GST fusion protein was eluted from the resin, and glutathione was removed by desalting to allow a solution-phase interaction assay (17). Protein interaction assays and immunoblotting were performed as described previously (17, 29).

Cell Culture and Transfection

COS7 or HEK293 cells were cultured and transfected as described previously (17). In brief, cells were suspended at 0.5–1.0 × 10^5 cells/ml, and 1.0 (12-well plate), 2.0 (35-mm dish), or 10 ml (100-mm dish) was plated. After 18 h, cells were transfected with 2 (12-well plate), 4–5 (35-mm dish), or 12 μg (100-mm dish) of cDNA with Lipofectamine 2000 (Invitrogen) as recommended by the manufacturer. For each experiment, transfection efficiency was monitored by pEGFP vector transfection to generate a fluorescent signal and immunoblotting. The transfection efficiency was 60–80%. Cell lysis and fractionation were performed as described previously (17, 30).

Transfection of Small Interfering RNA (siRNA) to Cultured Cardiomyocytes

Double strand siRNA oligonucleotides to rat *GNA15* ($G\alpha_{16}$; NCBI Reference Sequence NM_053542) and *TFE3* (NCBI Reference Sequence XM_228760) were synthesized (Stealth siRNA, Invitrogen) as follows: GNA15 siRNA: sense, 5′-CCAUGCAGGCCAUGAUUGAAGCAAU-3′; TFE3: sense, 5′-CAGAAGAAAGACAAUCACAACCUAA-3′. The conditions and duplex eliciting the most effective reduction in GNA15 and TFE3 were determined in a series of preliminary experiments. Cardiomyocytes were prepared from the hearts of 1–3-day-old Wistar rats as described previously (24). Approximately 24 h after preparation, neonatal cardiomyocytes at 4.0 × 10^5 cells in 35-mm plates were transfected with siRNA using Lipofectamine 2000 according to the manufacturer's instructions. Briefly, GNA15siRNA and TFE3siRNA individually in 50 μl of Opti-MEM I medium (Invitrogen) and 2.5 μl of Lipofectamine 2000 in 50 μl of Opti-MEM I medium were mixed, and then the mixture was added to cardiomyocytes. The final concentrations of GNA15siRNA and TFE3siRNA were 50 and 100 nM, respectively. The transfection efficiency of FITC-labeled oligonucleotide was 70–80%. The decrease of mRNA of GNA15 or TFE3 was confirmed by real time PCR following transfection of siRNAs.

Immunoprecipitation

Cell lysates were prepared in 250–500 μl of immunoprecipitation buffer (50 mM Tris, pH 7.4, 70 mM NaCl, 5 mM EDTA, 1% IGEPAL CA-630 (Sigma), and a protease inhibitor mixture (Complete Mini, Roche Applied Science)). The lysates were incubated with 1.0–3.5 μg of antibody for 18 h after preclearing with 25 μl of 50% Sepharose-G for 1 h at 4 °C. The samples were incubated with 25 μl of 50% Sepharose-G for 1 h at 4 °C, and the pellets were washed three times with immunoprecipitation buffer. Proteins were eluted in 30 μl of 2× Laemmli buffer and resolved by SDS-PAGE (24).

Measurements of Inositol Phosphates

COS7 cells were seeded in 12-well plates at 0.5–1.0 × 10^5 cell/well. Next, 40 h after transfection, the cells were washed three times with phosphate-buffered saline (PBS) and incubated with serum-free Dulbecco's modified Eagle's medium for 4 h. The amount of cellular inositol monophosphate was determined by IP-One ELISA (Cisbio) according to the manufacturer's protocol.

Immunocytochemistry

Tissue Sections—Mouse heart was fixed in 4% paraformaldehyde and embedded in paraffin. Sections (4 μm thick) were prepared after being deparaffinized with xylene and graded ethanol. Sections were incubated in 0.3% H_2O_2 in methanol for 30 min to inactivate endogenous peroxidases and then rinsed three times for 5 min each with PBS. Tissues were incubated in citrate buffer (pH 6.0) at 100 °C for 10 min. Tissues were blocked in 5% skim milk for 30 min at room temperature and then incubated overnight with goat anti-claudin 14 (ab19035, Abcam; 1:100) antibodies at 4 °C in a humidified chamber. After washing three times for 5 min each in PBS, tissues were processed by the avidin-biotin complex method using a commercially available kit (Vector Laboratories, Burlingame, CA) according to the manufacturer's instructions. Immunocomplexes were visualized with 3,3′-diaminobenzidine tetrahydrochloride (DAB) (Dako, Glostrup, Denmark) or with the Liquid DAB-Black Substrate kit (Zymed Laboratories Inc., San Francisco, CA).

Cultured Cells—Cells were seeded on 24 × 24-mm polylysine-coated coverslips. Cells were fixed with PBS containing 4% paraformaldehyde and 4% sucrose for 15 min and then incubated with 0.2% Triton X-100 in PBS for 5 min. After three washes with PBS, cells were incubated with 5% normal donkey serum in PBS for 1 h. Cells were incubated with primary antibodies for 18 h at 4 °C followed by incubation for 1 h with secondary antibody (goat anti-mouse Alexa Fluor 488 or goat anti-rabbit Alexa Fluor 594, highly cross-absorbed; Molecular Probes) diluted to 1:2000 in PBS. All antibody dilutions were centrifuged at 12,000 × *g* for 15 min prior to use. In some cases, cells were incubated with 1 μg/ml 4′,6′-diamidino-2-phenylindole, dihydrochloride (DAPI) (Molecular Probes) in PBS for 5 min after incubation with secondary antibodies. Slides were then mounted with glass coverslips with ProLong Gold antifade reagent (Invitrogen). Images were analyzed by deconvolution microscopy (TE2000-E, Nikon, Tokyo, Japan). Obtained images were deconvoluted using NIS-Elements 3.0 software (Nikon) with a "no neighbors" deconvolution algorithm. All images were obtained from approximately the middle plane of the cells.

TABLE 1

AGS cDNAs isolated from cardiac hypertrophy model of mouse

AGSs are numbered according to the order in which they were isolated from a functional screen in yeast. GPR, G-protein-regulatory motif. The number of transformants screened for each cDNA library of the heart is as follows: transverse aortic constriction, 1.6×10^7; isoproterenol infusion, 2.0×10^7.

Gene in database	AGS	Cardiac dysfunction model used to generate cDNA libraries for functional screen[a]	
		Transverse aortic constriction	Isoproterenol infusion
Dynlt1b (the entire coding sequence)	AGS2	+	−
GPSM1 (C-terminal 178 amino acids with 3 GPR motifs)	AGS3	+	−
RGS12 (C-terminal 206 amino acids with GPR motif)	AGS6	+	+
TFE3 (C-terminal 533 amino acids)	AGS11	+	+
TFEB (C-terminal 320 amino acids)	AGS12	−	+
MITF (C-terminal 304 amino acids)	AGS13	+	+

[a] cDNA libraries were screened in yeast strains CY1141 ($G\alpha_{i3}$), CY8342 ($G\alpha_s$), and CY9603 ($G\alpha_{16}$).

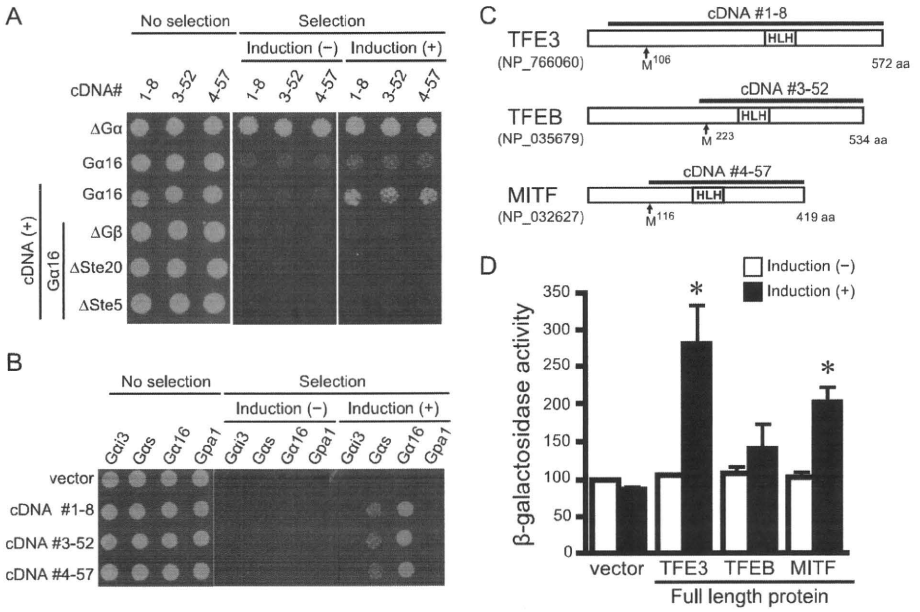

FIGURE 1. **Bioactivity and diagram of AGSs isolated from mouse hypertrophic heart.** In *A* and *B*, data are presented in three panels to illustrate the viability of the transformed yeast and the galactose-dependent growth under the selective pressure of exclusion of histidine from the medium. Galactose promotes the expression of each cDNA in the pYES2-containing *GAL1* promoter. About 2000 cells were suspended in H_2O and spotted on medium with glucose plus histidine (*left*; no selection), glucose minus histidine (*center*; selection without induction), or galactose plus histidine (*right*; selection plus induction). *A*, epistasis analysis of isolated clones. Transformants in a yeast strain expressing human $G\alpha_{16}$ (Gpa1(1–41)) and yeast lacking Gα, Gβ, or downstream signaling molecules (*ΔGα*, yeast lacking Gα; *ΔGβ*, yeast lacking Gβ; *ΔSte20*, yeast lacking p21-activated kinase; *ΔSte5*, yeast lacking the kinase scaffold protein). *B*, effect of isolated cDNAs in yeast expressing various types of Gα. *C*, schematic diagram of the sequences of TFE3, TFEB, and MITF in mouse. The *line above* the sequence refers to cDNA isolated by the yeast-based functional screen. *HLH*, helix-loop-helix. *D*, bioactivity of full-length TFE3, TFEB, and MITF. The full-length clones were transformed into yeast expressing $G\alpha_{16}$. The magnitude of activation of G-protein signaling pathway was monitored by β-galactosidase activity. Data are presented as the mean S.E. of five experiments with duplicate determinations. *, $p < 0.05$ *versus* non-induction group.

Miscellaneous Procedures and Statistical Analysis

Immunoblotting and data analysis were performed as described previously (18, 24). The luminescence images captured with an image analyzer (LAS-3000, Fujifilm, Tokyo, Japan) were quantified using Image Gauge 3.4 (Fujifilm). Data are expressed as mean ± S.E. from independent experiments as described in the figure legends. Statistical analyses were performed using the unpaired *t* test, F-test, and one-way analysis of variance followed by Tukey's multiple comparison post hoc test. All statistical analyses were performed with Prism 4 (GraphPad Software).

RESULTS

Identification of Activators of G-protein Signaling from Hypertrophied Hearts—We utilized an expression cloning system in *S. cerevisiae* to identify receptor-independent activators of G-protein signaling involved in the development of cardiac hypertrophy (18, 26). The yeast strains used in this screen system lacked the pheromone receptor but expressed mammalian Gα ($G\alpha_{i3}$, $G\alpha_s$, or $G\alpha_{16}$) in place of the yeast Gα subunit and provided a readout of growth upon activation of the G-protein-regulated pheromone signaling pathway. cDNA libraries from the left ventricle of the hypertrophy models were constructed in a galactose-inducible vector and introduced into these yeast strains. Functional screening for receptor-independent AGS proteins was then facilitated by selection of colonies growing in a galactose-specific manner.

We used two models of cardiac hypertrophy: the TAC-induced pressure overload model and the isoproterenol-induced tachycardiac hypertrophic model (supplemental Fig. 1). cDNA libraries from each model were introduced into the yeast strains expressing mammalian $G\alpha_{i3}$, $G\alpha_s$, or $G\alpha_{16}$ (Table 1). Twenty-

nine cDNA clones encoding six distinct proteins were isolated from the two cDNA libraries ($G\alpha_s$ strain, 0; $G\alpha_{i3}$ strain, 20; $G\alpha_{16}$ strain, 9). Each clone was retransformed into yeast to confirm plasmid-dependent growth, and then epistasis analysis was performed to identify the site of action within the pheromone pathway. Epistasis analysis demonstrated that six of these cDNA clones required G-protein to activate the growth-linked G-protein pathway, and thus these clones satisfied the definition of AGS (3, 27) (Table 1 and Fig. 1*A*).

Three clones isolated from yeast expressing $G\alpha_{i3}$ encoded the previously characterized proteins AGS2 (*Dynlt1b*, NCBI Reference Sequence NM_033368), AGS3 (*GPSM1*, NCBI Reference Sequence NM_700459), and AGS6 (*RGS12*, NCBI Reference Sequence NM_001156984). The cDNAs encoding AGS3 and AGS6 contained the G-protein-regulatory motif(s) that stabilizes the GDP-bound conformation of $G\alpha_i$, transducin, and $G\alpha_o$. An additional three cDNAs (1-8, 3-52, and 4-57) were isolated from yeast expressing $G\alpha_{16}$. These three cDNAs exhibited bioactivity in yeast strains expressing $G\alpha_{16}$ but not in yeast expressing $G\alpha_{i3}$, $G\alpha_s$, or Gpa1 (yeast $G\alpha$), indicating $G\alpha$ selectivity (Fig. 1*B* and supplemental Text 1). We therefore focused on these $G\alpha_{16}$-specific AGS cDNAs.

$G\alpha_{16}$-specific AGS Proteins—Sequence analysis of the $G\alpha_{16}$-specific cDNAs indicated that all encoded MITF/TFE transcription factors (31–33). cDNA1-8 encoded the C-terminal 533 amino acids of TFE3 (NCBI Reference Sequence NP_766060), cDNA3-52 encoded the C-terminal 320 amino acids of TFEB (NCBI Reference Sequence NP_035679), and cDNA4-57 encoded the C-terminal 304 amino acids of MITF (NCBI Reference Sequence NP_032627) (Fig. 1*C*). In accordance with the numbering of previously discovered AGS proteins (18), cDNA1-8, cDNA3-52, and cDNA4-57 were termed AGS11, AGS12, and AGS13, respectively (Table 1).

Full-length TFE3, TFEB, and MITF were cloned into a yeast expression vector, and the bioactivity for the G-protein signaling pathway was determined by β-galactosidase reporter assays (Fig. 1*D*). Full-length TFE3 and MITF, but not TFEB, activated the G-protein pathway in $G\alpha_{16}$-expressing cells. Full-length TFE3, MITF, and TFEB did not activate growth of yeast expressing $G\alpha_s$ (supplemental Text 2). Immunoblot analysis indicated that the full-length proteins were expressed at the

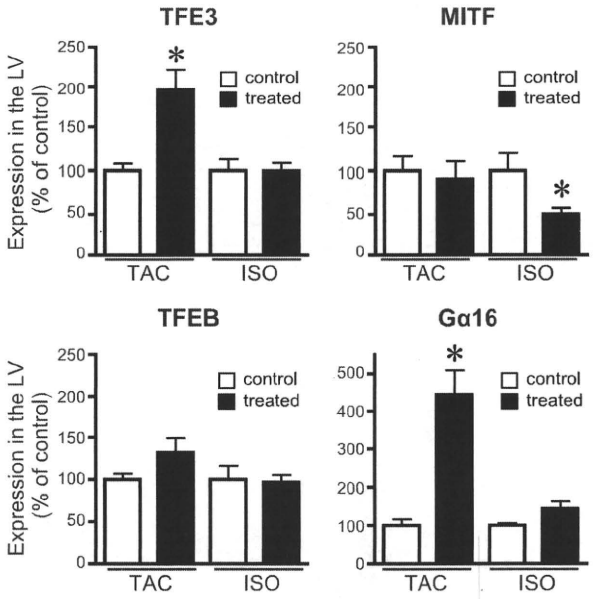

FIGURE 2. **Expression of MITF/TFE transcription factors and $G\alpha_{16}$ in mouse cardiac hypertrophy model.** The expression of mRNA of each gene was analyzed by real time PCR as described under "Experimental Procedures." *Control* refers to the sham-operated or saline-infused mouse. Data are expressed as the -fold change in level compared with the control group. *ISO*, continuous infusion of isoproterenol; *LV*, left ventricle. Data are presented as the mean ± S.E. of five experiments with duplicate determinations. *, $p < 0.05$ *versus* control group.

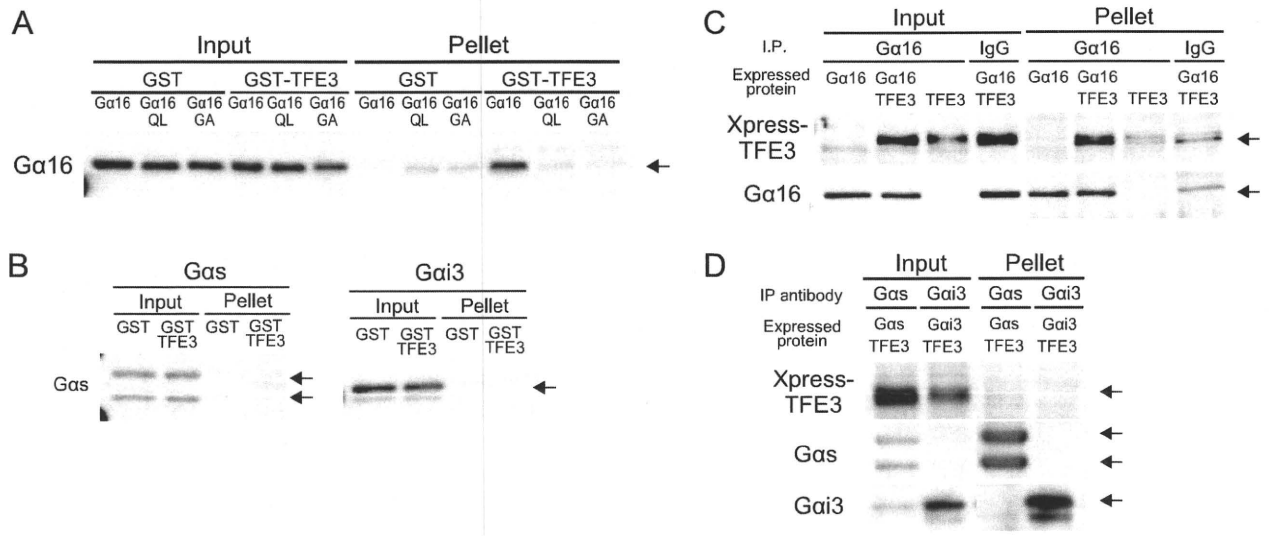

FIGURE 3. **Interaction of TFE3 with $G\alpha_{16}$ *in vitro* and in cell.** *A* and *B*, GST pulldown assay of TFE3 with COS7 lysate expressing various Gα subunits. The C-terminal 533-amino acid fragment of TFE3 was expressed as a GST fusion protein (GST-TFE3). GST-TFE3 (300 nM) was incubated with 1 mg of cell lysate in a total volume of 500 μl at 4 °C. Lysates of COS7 cells were prepared as described under "Experimental Procedures" following transfection of 10 μg of the Gα subunit in pcDNA3. *C* and *D*, COS7 cells in a 100-mm dish were transfected with a combination of pcDNA3, pcDNA3::$G\alpha_{16}$ (5 μg/dish), and pcDNA3.1-His::TFE3 (5 μg/dish). The amount of DNA transfected was adjusted to 10 μg/well with the pcDNA3 vector. The preparation of a whole-cell lysate including the nuclear fraction and immunoprecipitation (*IP*) were performed as described under "Experimental Procedures." The Gα subunit was immunoprecipitated with a specific antibody for each Gα subunit. *QL*, $G\alpha_{16}$Q212L; *GA*, $G\alpha_{16}$G211A.

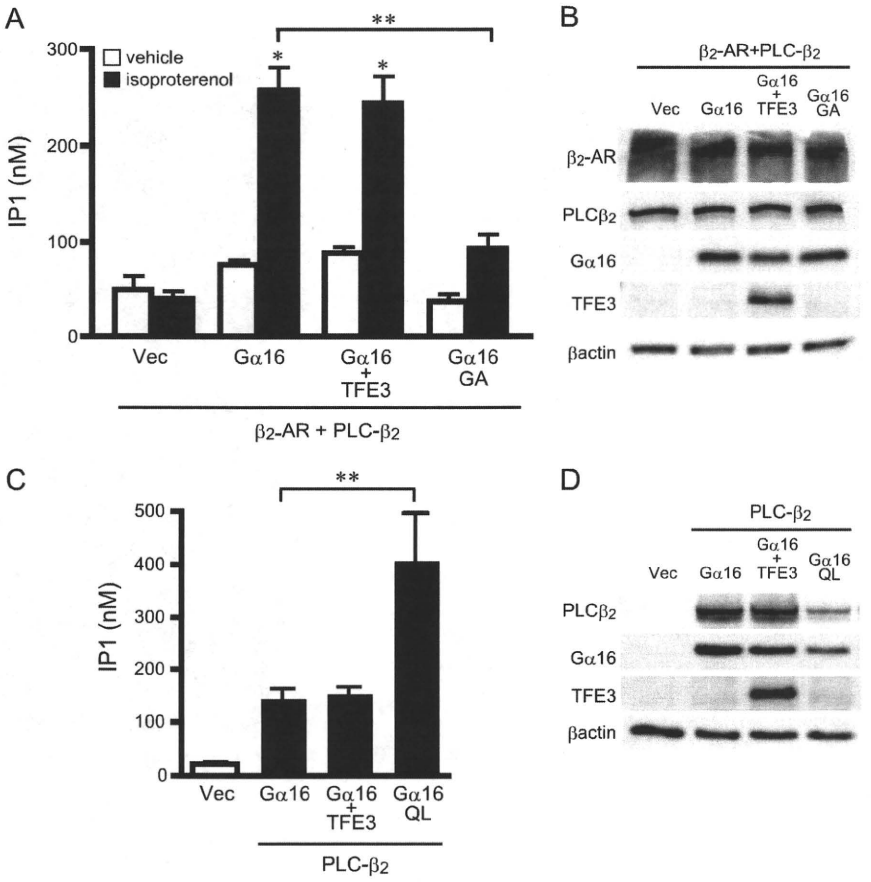

FIGURE 4. **Effect of TFE3 on activation of phospholipase C-β2.** *A*, effect of TFE3 on the generation of inositol phosphate (*IP1*) following receptor stimulation. COS7 cells were transfected in 12-well plates with control vectors (*Vec*) or cDNAs as indicated (0.4 μg of pcDNA::PLC-β2, 0.5 μg of pcDNA::TFE3, 0.5 μg of pcDNA::$G\alpha_{16}$, and 0.6 μg of pEGFP::β_2-adrenergic receptor (*AR*)). The amount of transfected DNA was adjusted to 2 μg/well with the pcDNA vector. Cells were stimulated with 10 μM isoproterenol for 30 min and assayed immediately. Data are expressed as the mean ± S.E. of five experiments with duplicate determinations. *B*, expression of transfected proteins of *A*. The expression of each protein was determined by immunoblotting of 10 μg of whole-cell lysates. *C*, effect of TFE3 on the generation of inositol phosphate. COS7 cells were transfected in 12-well plates with control vectors or cDNAs as indicated (0.5 μg of pcDNA::PLC-β2, 0.75 μg of pcDNA::TFE3, and 0.75 μg of pcDNA::$G\alpha_{16}$). The amount of transfected DNA was adjusted to 2 μg/well with the pcDNA vector. Data are expressed as the mean ± S.E. of five experiments with duplicate determinations. *D*, expression of transfected cDNA of *C*. The expression of each protein was determined by immunoblotting of 10 μg of whole-cell lysates. *, $p < 0.05$ *versus* control group; **, $p < 0.05$ between two groups. *QL*, $G\alpha_{16}$Q212L; *GA*, $G\alpha_{16}$G211A.

expected size and that their expression did not alter the levels of $G\alpha_{16}$. These findings suggest that TFE3, MITF, and TFEB are transcription factors that act as receptor-independent G-protein activators. AGSs with various functions have been identified; however, no transcription factors have previously been described as AGS proteins.

Expression of TFE3, TFEB, and MITF in Cardiac Hypertrophy Models—It was reported previously that the expression level of MITF was associated with development of cardiac hypertrophy in mouse (34). We sought to determine whether the three $G\alpha_{16}$-specific AGS proteins were up-regulated in cardiac hypertrophy or were constitutively expressed in the myocardium. RNA expression of TFE3, MITF, TFEB, and the target $G\alpha_{16}$ subunit was determined in the hypertrophied myocardium (Fig. 2). TFE3 mRNA expression was up-regulated in the left ventricle in the TAC model but not in the isoproterenol model. MITF was unchanged in the TAC model but reduced in the isoproterenol model. TFEB did not show any significant changes of expression in either model. Notably, $G\alpha_{16}$ mRNA expression was also increased in the TAC model in which TFE3 was up-regulated. As TFE3 and $G\alpha_{16}$ were both significantly up-regulated in the TAC model, we focused on the characterization of TFE3.

Formation of TFE3-$G\alpha_{16}$ Complex in Cells—The above findings suggested that TFE3 plays an important role via $G\alpha_{16}$ in the development of cardiac hypertrophy. We thus examined whether TFE3 indeed was able to form a complex with $G\alpha_{16}$. As a first approach, the interaction of GST-tagged TFE3 (GST-TFE3) with $G\alpha_{16}$ was examined *in vitro*. GST-TFE3 successfully pulled down transfected $G\alpha_{16}$ from cell lysates. However, neither a constitutively active mutant of $G\alpha_{16}$ ($G\alpha_{16}$Q212L) nor an inactive mutant of $G\alpha_{16}$ ($G\alpha_{16}$G211A) was pulled down, suggesting that the interaction of $G\alpha_{16}$ and TFE3 was dependent upon the conformation of $G\alpha_{16}$ and regulated by guanine nucleotide binding (Fig. 3*A*) (35, 36). In contrast, GST-TFE3 did not pull down transfected $G\alpha_s$ or $G\alpha_{i3}$ from cell lysates (Fig. 3*B*). We also examined whether TFE3 interacted with $G\alpha_{16}$ in mammalian cells. Expressed TFE3 was co-immunoprecipitated with $G\alpha_{16}$ from COS7 cell lysates, suggesting that TFE3 and $G\alpha_{16}$ formed a stable complex

within these cells (Fig. 3*C*). In contrast, TFE3 did not co-immunoprecipitate with $G\alpha_s$ or $G\alpha_{i3}$ (Fig. 3*D*). We next examined the role of this interaction in $G\alpha_{16}$-mediated signaling events.

TFE3 Is Not Involved in Receptor-mediated $G\alpha_{16}$ Signaling—$G\alpha_{16}$ is coupled to multiple GPCRs including β_2-adrenergic receptors mediating signal transfer to the effector molecule PLC-β (37, 38). Thus, we examined whether TFE3 regulated β_2-adrenergic receptor-mediated PLC-β2 activation as a representative of $G\alpha_{16}$-mediated signaling (39). In a transient expression system in COS7 cells, $G\alpha_{16}$ activated PLC-β2 following β_2-adrenergic receptor stimulation as determined by inositol monophosphate production (Fig. 4). The magnitude of PLC-β2 activation was reduced in the presence of an inactive $G\alpha_{16}$ mutant ($G\alpha_{16}$G211A), indicating that PLC-β2 activation was mediated by $G\alpha_{16}$ (Fig. 4, *A* and *B*). However, TFE3 overexpression did not alter this receptor-mediated $G\alpha_{16}$ signaling. We also examined the effect of TFE3 overexpression on the basal activity of PLC-β2/$G\alpha_{16}$ in the absence of receptor stimulation. TFE3 overexpression did not alter PLC-β2 activity, whereas a constitutively active mutant of $G\alpha_{16}$ ($G\alpha_{16}$Q212L) increased the activity even in the absence of receptor stimulation (Fig. 4, *C* and *D*). These data are consistent with a lack of TFE3 involvement in regulating the conventional GPCR-mediated $G\alpha_{16}$ signaling pathway.

TFE3 Induces Accumulation of $G\alpha_{16}$ in Nucleus—The identification of transcription factors as $G\alpha_{16}$-specific AGS proteins suggested that MITF/TFE transcription factors may interact with a subpopulation of $G\alpha_{16}$ distinct from that involved in the conventional G-protein signaling at the plasma membrane. To address this issue, we first examined the subcellular distribution of $G\alpha_{16}$ and TFE3 when each was independently overexpressed in the cell. Overexpressed TFE3 was predominantly found in the nucleus as expected, whereas $G\alpha_{16}$ was found in the plasma membrane and cytoplasm but not in the nucleus (Fig. 5, *arrow*, and supplemental Fig. 2, A, B, and D). However, when $G\alpha_{16}$ and TFE3 were overexpressed together, $G\alpha_{16}$ predominantly accumulated in the nucleus (Fig. 5, *arrow*). This novel nuclear translocation of $G\alpha_{16}$ was not due to $G\alpha_{16}$ activation because the constitutively active mutant of $G\alpha_{16}$ ($G\alpha_{16}$Q212L) was not found in the nucleus when it was overexpressed by itself. These data suggested that $G\alpha_{16}$ forms a complex with TFE3 and translocates to the nucleus. Nuclear accumulation of G-protein by TFE3 was not observed for $G\alpha_{i3}$ or $G\alpha_s$.

Up-regulation of Claudin 14 mRNA by TFE3-$G\alpha_{16}$ Complex—The co-localization of TFE3 and $G\alpha_{16}$ suggested an involvement of a nuclear TFE3-$G\alpha_{16}$ complex in regulating the expression of particular genes. To address this issue, genes regulated by TFE3 and $G\alpha_{16}$ were screened by microarray analysis of mRNA of HEK293 cells transfected with TFE3 and/or $G\alpha_{16}$. In the screening of more than 40,000 human genes, we found that claudin 14 mRNA was highly up-regulated by the simultaneous transfection of TFE3 and $G\alpha_{16}$. Parallel experiments indicated that the co-overexpression of TFE3 and $G\alpha_{16}$ in HEK293 cells increased claudin 14 mRNA by 133-fold, whereas independent overexpression of TFE3 (8.3-fold) or $G\alpha_{16}$ (1.0-fold) had minimal effect on the induction of claudin 14 (Fig. 6*A*). The induction of claudin 14 was significantly decreased in the presence of the inactive mutant of $G\alpha_{16}$ ($G\alpha_{16}$G211A) compared with wild type $G\alpha_{16}$, suggesting that $G\alpha_{16}$ activation was also required for the induction of this gene.

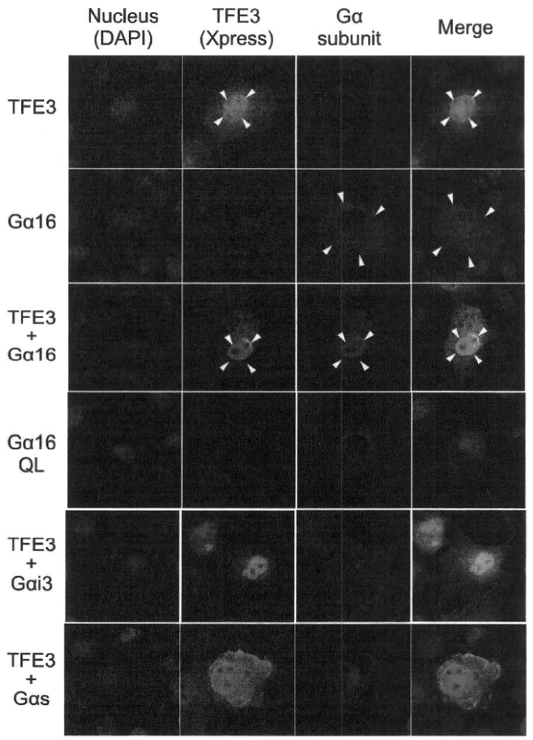

FIGURE 5. **Localization of expressed Gα subunits and TFE3 in COS7 cells.** COS7 cells were transfected in a 35-mm dish with 2.0 μg of Gα subunits in pcDNA3 and/or 2.0 μg of pcDNA3.1-His::TFE3. The amount of transfected DNA was adjusted to 4 μg/well with the pcDNA3 vector. The Gα subunit and TFE3 were determined using a specific antibody for each Gα (*red*) or Xpress antibody (*green*), respectively. *QL*, $G\alpha_{16}$Q212L.

Requirement of $G\alpha_{16}$ Activation for Gene Induction by TFE3—The requirement of $G\alpha_{16}$ activation for this gene induction was further characterized utilizing a truncated mutant of TFE3 (delTFE3), which showed less bioactivity for $G\alpha_{16}$ activation in the yeast system. Analysis of the amino acid sequences of the MITF/TFE family indicated that the C-terminal 27 acids were conserved among the $G\alpha_{16}$-selective AGS proteins (Fig. 6*B*, *upper panel*). Deletion of the C-terminal 27 amino acids resulted in the loss of bioactivity of TFE3 and MITF for G-protein activation (Fig. 6*B*, *left middle panel*, and supplemental Text 3). Despite the loss of bioactivity for $G\alpha_{16}$ activation, delTFE3 was still able to form a complex with $G\alpha_{16}$ and induce the translocation of $G\alpha_{16}$ to the nucleus (Fig. 6*B*, *left lower* and *right panels*, and supplemental Fig. 2, C and D). Thus, nuclear translocation by itself did not require $G\alpha_{16}$ activation as long as TFE3 and $G\alpha_{16}$ formed a complex (Fig. 6*A*).

Although the delTFE3-$G\alpha_{16}$ complex was found in the nucleus, the subsequent up-regulation of claudin 14 was blunted, suggesting that $G\alpha_{16}$ activation is critical for this gene induction (Fig. 6*A*). Furthermore, the constitutively active mutant of $G\alpha_{16}$ ($G\alpha_{16}$Q212L), which was not expressed in the nucleus (Fig. 5), failed to induce claudin 14. MITF, which had a similar ability to activate $G\alpha_{16}$ (Fig. 1*D*), failed to induce claudin